Supplemental Materials

Molecular Biology of the Cell

Antoniali et al.

SIRT1 gene expression upon genotoxic damage is regulated by APE1 through nCaRE-promoter elements

Giulia Antoniali[a], Lisa Lirussi[a], Chiara D'Ambrosio[b], Fabrizio Dal Piaz[c], CarloVascotto[a], Elena Casarano[a], Daniela Marasco[d,e], Andrea Scaloni[b], Federico Fogolari[a] and Gianluca Tell[a,#]

[a] Department of Biomedical Sciences and Technologies, University of Udine, 33100 Udine, Italy;

[b]Proteomics & Mass Spectrometry Laboratory, ISPAAM, National Research Council, 80147 Naples, Italy;

[c] Department of Biomedical and Pharmaceutical Sciences, University of Salerno, 84084 Fisciano (Salerno), Italy;

[d] Department of Biological Sciences, University of Naples "Federico II", 80134 Naples, Italy;

[e] Institute of Biostructures and Bioimaging, National Research Council, 80134 Naples, Italy

SUPPLEMENTAL MATERIAL

List of contents:

Supplemental Results

Limited proteolysis analyses

A combined limited proteolysis-mass spectrometry analysis was carried out to investigate the APE1 protein region responsible for the nCaRE binding. Experiments were performed on a recombinant APE1 form bearing three additional amino acids at protein N-terminus with respect to the native counterpart. Panels *I* and *IV* of Figure S5 show the time-course LC-ESI-MS analysis of the endoprotease AspN digestion performed on isolated APE1, as carried out by using an enzyme/substrate of 1:500 w/w. Under these experimental conditions, APE1 remained partly undigested, showing that its native conformation is susceptible to proteolysis at a unique, likely flexible site. After 5 min, only the peptide pair 1-17 and 18-321 was detected (Figure S5, *panel I*), and no further fragments were released after 60 (Figure S5, *panel IV*) and 120 min (data not shown) (Supplemental Table S4). As previously reported (Scaloni *et al.*, 1999), the definition of the primary cleavage sites was inferred by the identification of the complementary peptides released by a single proteolytic event occurring on the intact protein. According to these criteria, non-complexed APE1 was preferentially cleaved at D18 present within the unstructured protein N-terminal domain. When the APE1-SIRT1 nCaRE-B oligonucleotide complex was analyzed under the same conditions, no proteolytic fragments resulting from D18 cleavage were released even after 60 min (Figure S5, *panel II* and *V*) (Supplemental Table S4), demonstrating a tighter conformation of the complex and a DNA-shielding effect for D18. A significantly reduced digestion product at this site was observed only after incubation for 120 min (data not shown). A similar result was obtained also for the APE1-PTH nCaRE-B oligonucleotide complex, which showed absent or negligible proteolysis at D18 after 5 and 60 min, respectively (Figure S5, panel *III* and *VI*). These results clearly demonstrate that upon APE1 interaction with DNA, D18 is no longer accessible to the protease action. Thus, it may be hypothesized that this residue is placed at the protein-nCaRE oligonucleotide complex interface.

The different accessibility of the basic residues in the isolated APE1 protein and in its complex with nCaRE-B oligonucleotides was similarly probed with trypsin, used at 1:5000 w/w enzyme/substrate (Supplemental Table S4). LC-ESI-MS analysis of the proteolytic fragments, released from the isolated protein, led to the identification of the complementary peptide pairs 1-9, 10-321 and 1-10, 11-321 already after 5 min of reaction, which were generated by single hydrolytic events at K9 and K10, respectively. Additional products, resulting from fragment subdigestion reactions, were also observed, but they did not provide information on further accessible amino acids. These results confirmed that APE1 N-terminal portion is very flexible and highly exposed to the proteolytic action. Conversely, appreciable hydrolysis of recombinant APE1 following protein interaction with SIRT1 nCaRE-B or APE1-PTH nCaRE-B oligonucleotides was observed at K9 only after 60 min of reaction (Supplemental Table S4). Due to the nature of the proteolytic products observed, these experiments confirmed the masking effect of both oligonucleotides over the non-structured protein N-terminal region.

Further experiments were then carried out with broader-specificity proteases, such as chymotrypsin and elastase. In the first case, limited proteolysis of isolated APE1 (enzyme/substrate of 1:1000 w/w) generated only a complementary peptide pair, namely 1-114 and 115-321, which identified L114 as the primary cleavage site (Supplemental Table S4). Additional products resulting from fragment subdigestions were also observed, but they did not provide information on further accessible amino acids. According to X-ray crystallographic data, this residue is exposed on the molecular surface of the globular APE1 domain (Gorman *et al.*, 1997). No significant differences were observed on a time-course basis when peptide maps were characterized for both APE1-nCaRE oligonucleotide complexes (Supplemental Table S4). In fact, both peptides 1-114 and 115-321 were

detected within the APE1-SIRT1 nCaRE-B and APE1-PTH nCaRE-B oligonucleotide products after 5 and 15 min, respectively, similarly to the non-complexed protein sample. These data excluded any involvement of L114 in binding to the nCaRE-B elements and further confirmed the suitability of the strategy used here.

When elastase digestion of isolated APE1 was carried out using an enzyme/substrate of 1:1000 w/w, only two peptide pairs (1-12, 13-321, and 1-14, 15-321) were detected after 5 min of reaction, whereas an additional pair (1-20, 21-321) was observed after 15 min (Supplemental Table S4). These data demonstrated that non-complexed APE1 was preferentially cleaved at A12, A14 and L20. When the recombinant APE1-SIRT1 nCaRE-B oligonucleotide and APE1-PTH nCaRE-B oligonucleotide complexes were analyzed under the same conditions, different proteolytic patterns were obtained, which proved preferential cleavage site at L20, as demonstrated by the identification of the complementary peptides 1-20 and 21-321 after 30 min of reaction (Supplemental Table S4). These results clearly demonstrated that, upon complex formation, A12 and A14 are no longer accessible to elastase, whereas L20 is still partially exposed to the protease action.

Supplemental Figure Legends

Supplemental Figure S1.
Schematic representation of the pipeline steps used for the identification of putative nCaRE-B elements within the human genome.

Supplementary Figure S2.
To test the binding affinity of APE1 for SIRT1 nCaRE sequence, a comparative analysis between the mutated nCaRE sequence and a polyT sequence was performed using SPR. Overlay of sensorgrams relative to the binding of APE1 to immobilized biotinylated ds oligonucleotide corresponding to polyT (A) and nCaRE SIRT1-B (B) and nCaRE SIRT1-B mutated sequence (C). APE1 concentration ranged within 1.0-20 μM for nCaREs and 1.0-10μM for polyT .

Supplemental Figure S3.
To demonstrate that Ku70 is able to stabilize the binding ability of APE1 to SIRT1-B nCaRE sequence we performed EMSA analysis with ds oligonucleotide corresponding to nCaRE SIRT1-B sequence with $APE1^{WT}$ and Ku70 purified recombinant protein. Reactions were performed with 2.5 pmol of nCaRE SIRT1-B oligonucleotide and 10, 20 or 30 pmol of $APE1^{WT}$ (lanes 2, 3, 4), Ku70 (lanes 5, 6, 7) and both $APE1^{WT}$ and Ku70 (lanes 8, 9, 10). Lane 1 represents probe alone; F shows the position of the free oligonucleotide probe. Specific protein/nCaRE interaction is indicated by the arrow. Notably, Ku70 is unable per se to directly bind the SIRT-1 B sequence but significantly enhances APE1 DNA binding activity on this sequence.

Supplemental Figure S4.
To corroborate structural data obtained for SIRT1-B nCaRE-B sequence with T7 endonuclease we performed the same experiment with another enzyme, the mung bean nuclease (Amosava *et al*., 2011), a single-strand specific endonuclease, typically used for the removal of hairpin loops during cDNA synthesis. (A) EMSA analysis with APE1 on SIRT1 nCaRE-B after mung bean endonuclease digestion. 2.5 pmol of ds oligonucleotide corresponding to nCaRE SIRT1-B were digested with mung bean endonuclease at 30°C for the indicated period of time. The reactions then were incubated at 37°C with 10 pmol of recombinant APE1 protein for additional 15 min. Lanes 1 is probe alone; F shows the position of the free oligonucleotide probe. Specific APE1/nCaRE interaction is indicated by arrow. (B) APE1 and mung bean endonuclease compete for the same nCaRE binding site. EMSA analysis of APE1 binding to nCaRE sequence after digestion with mung bean endonuclease or after preincubation with APE1 and subsequent digestion with mung bean. 2.5 pmol of ds oligonucleotide corresponding to nCaRE SIRT1-B were first digested with mung bean endonuclease at 30°C for 4 h and subsequently incubated with increasing amounts of recombinant APE1 (10, 30 pmol) at 37°C for 15 min (lanes 7, 8). Alternatively, 2.5 pmol of SIRT1-B nCaRE probe were first incubated with APE1 at 37°C for 15 min and sequentially digested at 30°C for 4 h with mung bean endonuclease (lanes 9, 10). Lanes 1 is probe alone; 1^{st} and 2^{nd} indicate if APE1 incubation with the probe was performed temporally before (1^{st}) or after (2^{nd}) mung bean digestion; F shows the position of the free oligonucleotide probe. Specific APE1/nCaRE interaction is indicated by arrow.

Supplemental Figure S5.
Comparative limited proteolysis experiments on isolated or DNA-complexed APE1. Time-course analysis of simultaneous trials performed on non-complexed recombinant APE1 (I, IV), recombinant APE1-SIRT1 nCaRE-B complex (II, V) or recombinant APE1-PTH nCaRE complex (III, VI) are shown. LC-ESI-MS profiles from samples taken at 5 (I-III) and 60 min (IV-VI) are reported. Identified peptides are reported on the corresponding chromatographic peaks; 1-321 denotes the intact protein. See Supplemental Table S4 for detailed information. Experiments were

performed on a recombinant APE1 form bearing three additional amino acids at protein N-terminus with respect to the native counterpart.

Supplemental Figure S6.

To determine the optimal time for a detectable SIRT1 mRNA and protein accumulation upon 1 mM H_2O_2 treatment, we harvested cells at different time of release as indicated. (A) Data shown in the histogram represent the amount of SIRT1 mRNA normalized to the amount of GAPDH. Statistical tests were estimated by Student's t test. A p-value < 0.001 was considered as statistically significant (*). (B) The induction of SIRT1 protein levels were estimated in HeLa cells treated with 0.1 mM H_2O_2 for the indicated times. SIRT1 protein levels were measured on whole cell lysate (WCE) using a specific antibody; tubulin was used as a loading control. Histogram reports the densitometric quantification of Western blotting signals from at least three independent replicates. SIRT1 amounts are expressed as mean ± SD of the signal, considering the untreated sample as reference. A *p*-value < 0.05 was considered as statistically significant (*). (C) To finally corroborate our model of SIRT1 activation after oxidative treatment, the p53 acetylation status of K382, a known target of SIRT1 deacetylation (Vaziri *et al*., 2001), has been estimated. Western blotting analysis of SIRT1 protein levels and of p53 acetylation in clones expressing $APE1^{WT}$, APE1 silenced cells $APE1^{CL.3}$ and control clones $APE1^{SCR-1}$ after 1 mM H_2O_2 treatment, for 1 h. Data shown in the histogram are normalized to the amount of tubulin and represent the densitometric quantification of SIRT1 protein level and of p53 acetylation. Data are expressed as average fold of induction relative to the untreated cells in at least three independent Western blotting analysis.

Supplemental Figure S7.
Recruitment of BER enzymes on hSIRT1 promoter after oxidative condition. HeLa cells treated with 1 mM H_2O_2 for 10, 15, 20, 40, 60 minutes, were analyzed by qChIP using specific antibodies recognizing 8-oxodG, OGG1 and APE1. The histogram represent the amount of hSIRT1 promoter sequence immunoprecipitated. Data were presented as percent of input and normalized to the quantity of DNA immunoprecipitated by α-tubulin (α-tub) and further normalized on the amount of immunoprecipitated protein.

Supplemental Figure S8.
Time-course interaction of RNA Polymerase II and Ku70 with APE1 after H_2O_2 treatment. HeLa cells were transfected with a plasmid expressing $APE1^{WT}$ and challenged with 1 mM H_2O_2, for different times (as reported). Immunoprecipitated material and whole cell lysate were separated onto SDS-PAGE, immunoblotted and analyzed for their Ku70 (*upper panel*) and RNA Polymerase II (*bottom panel*) content, as associated with APE1 after H_2O_2 stimulus. Ponceau S staining was used for loading control. Normalized co-immunoprecipitated amounts of Ku70 and RNA Polymerase II are indicated under each relative bar. Mean values of two independent experiments are reported for Ku70.

Supplemental Figure S9.
To further support the evidences of SIRT1 mRNA and protein induction upon oxidative stress (H_2O_2), we also challenged the cells with another genotoxic agent, methyl methanesulfonate (MMS). (A) Analysis of SIRT1 mRNA level with Q-PCR in clones expressing $APE1^{WT}$ or APE1 silenced cells $APE1^{CL.3}$ after 0.5 mM MMS treatment for 8 h. Data shown in the histogram are normalized to the amount of GAPDH. The significance of sample average difference observed was estimated with Schaffè test. A p-value < 0.05 was considered as statistically significant (*). Below, Western blotting analysis on protein extract of clones used. Tubulin protein level was used to normalize sample. (B) HeLa cells were treated with 0.5 mM MMS for the indicated times. SIRT1 protein levels were measured on whole cell lysate (WCE) using a specific antibody; tubulin was

used as a loading control. Histogram reports the densitometric quantification of Western blotting signals from at least three independent replicates. SIRT1 amounts are expressed as mean ± SD of the signal, considering the untreated sample as reference. A *p*-value < 0.05 was considered as statistically significant (*).

Supplemental Table Legends

Supplemental Table S1.
Significant GO terms associated to genes bearing nCaRE elements and present in expression profile data obtained from experiment in which APE1 was knocked down. Here we are reported only the most significant GO annotation terms obtained when performing the exact Fisher's test. The column titled “n_annotation” correspond to the total number of genes associated to that GO term in Gene Ontology database; instead, column “n_both” represents the amount of genes in our dataset associated to the same GO term. “Expect” column reports for all GO terms the number of genes expected by chance in a set made of the same number of dataset genes, but selected at random from database. The columns titled “C”, “F” and “P” correspond to the three branches of the Gene Ontology: cellular component, molecular function and biological process respectively.

Supplemental Table S2.
The final 57 genes extracted from the application of Gene Ontology and phylogentic footprinting analysis that can be considered *bona fide* as bearing the candidate nCaRE sequences within their regulatory elements and potentially regulated by APE1.

Supplemental Table S3.
Complete data reporting all the significant functional enrichments obtained performing GeneCodis analysis. ‘GO term ID’ and ‘Annotations’ columns represent the Gene Ontology codes of annotations and the textual description of annotations, respectively. BP refers to ‘biological process’ category of Gene Ontology annotation. Third and fourth columns represent the number of genes in the input list and the reference list for a given annotation, respectively. P-values calculated using hypergeometric distribution and its correction using the stimulation-based approach are reported. The ‘Genes’ column identifies the set of genes in the input list showing a given annotation.

Supplemental Table S4.

Comparative limited proteolysis experiments on isolated or DNA-complexed APE1. Experiments were performed on a recombinant APE1 form bearing three additional amino acids at protein N-terminus with respect to the native counterpart. Time-course analysis of simultaneous trials performed on non-complexed recombinant APE1, recombinant APE1-SIRT1 nCaRE-B complex or recombinant APE1-PTH nCaRE complex are shown. Proteolytic enzyme, protein to protease ratio (w/w), sampling time, peptide, theoretical and experimental mass value, and primary cleavage site in the recombinant and the native protein (in parenthesis) are shown.

Supplemental Figures

Supplemental Figure S1

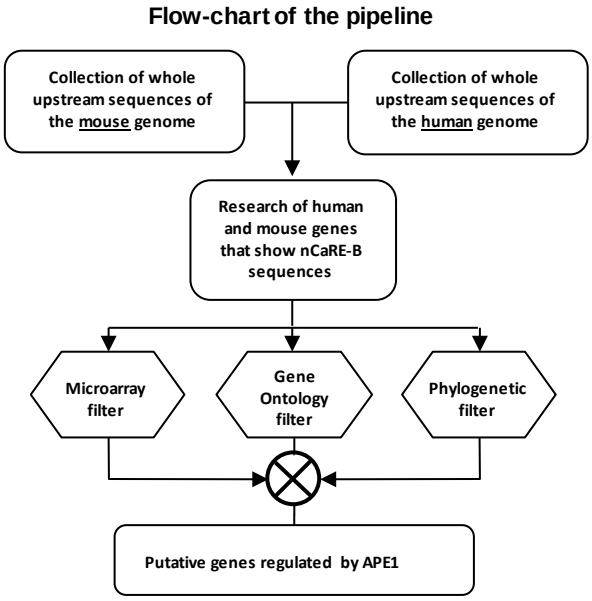

Supplemental Figure S2

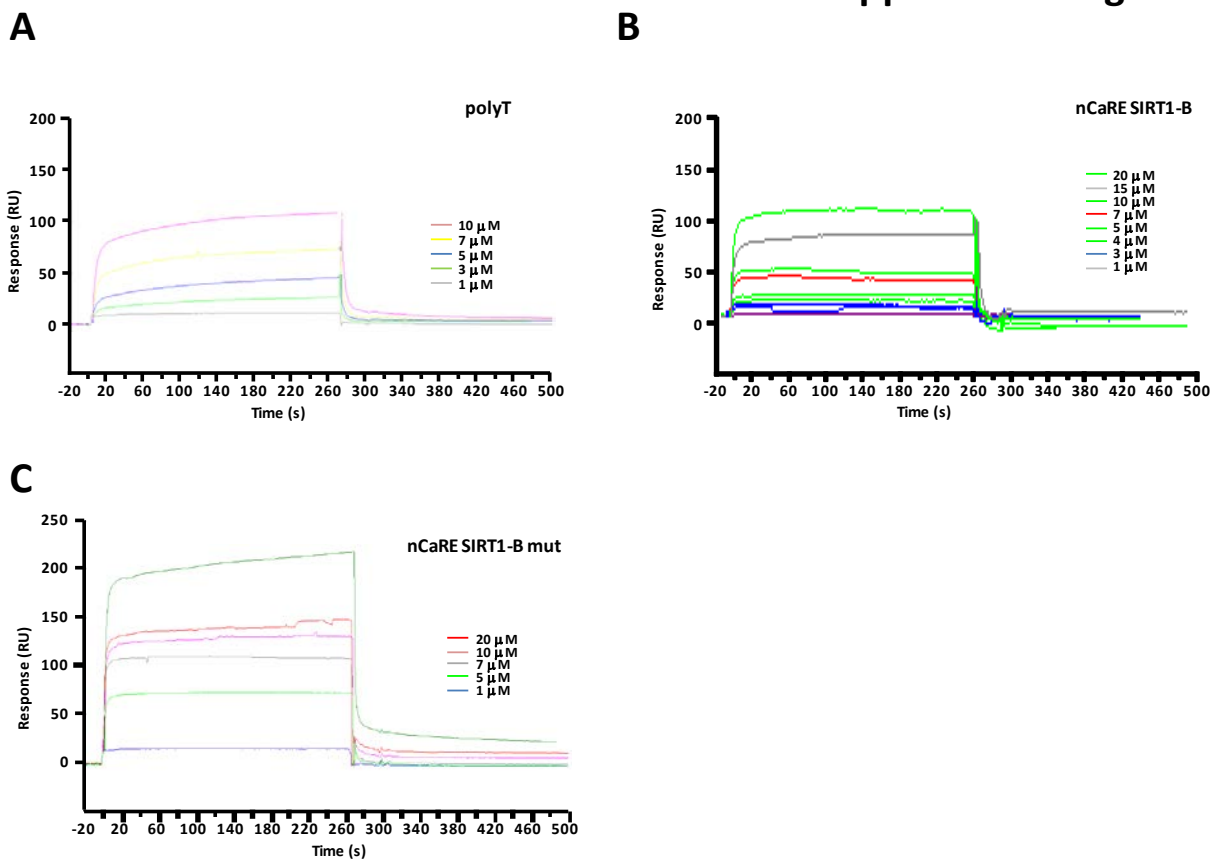

Supplemental Figure S3

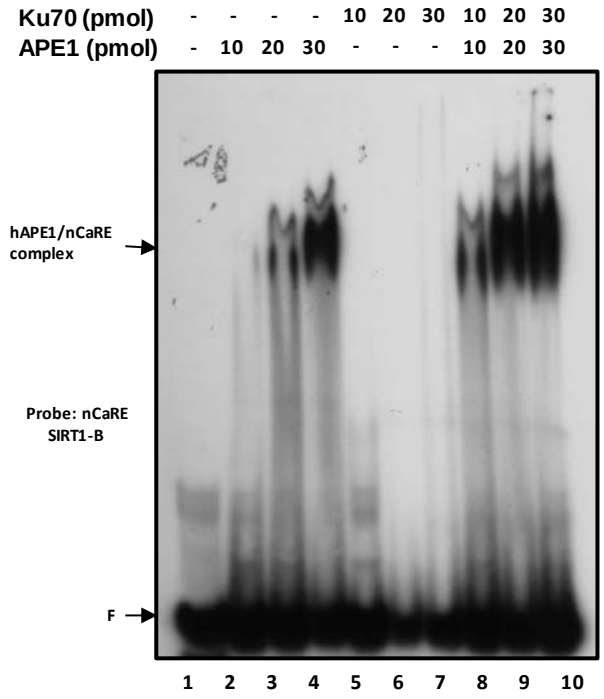

Supplemental Figure S4

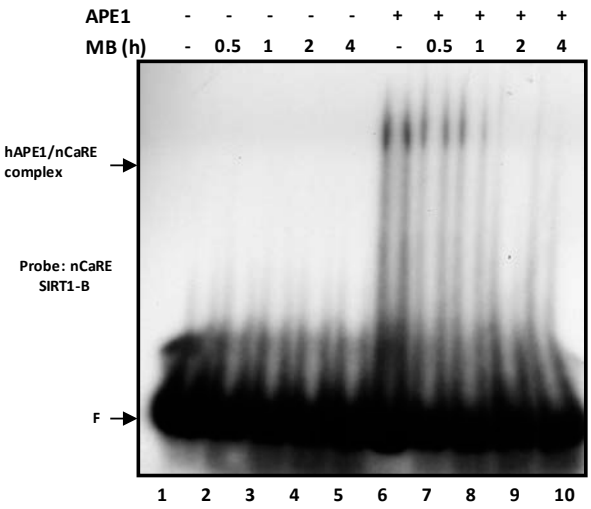

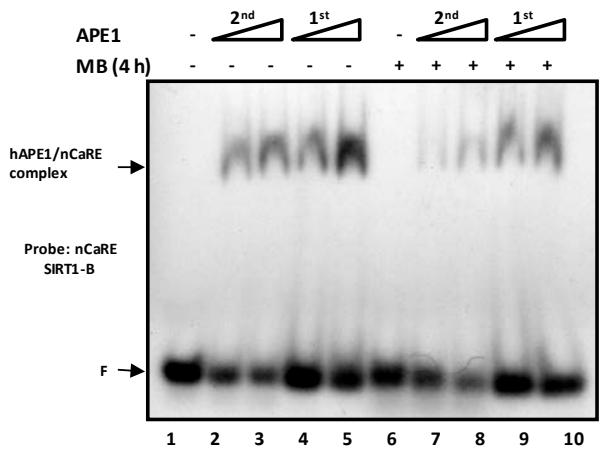

Supplemental Figure S5

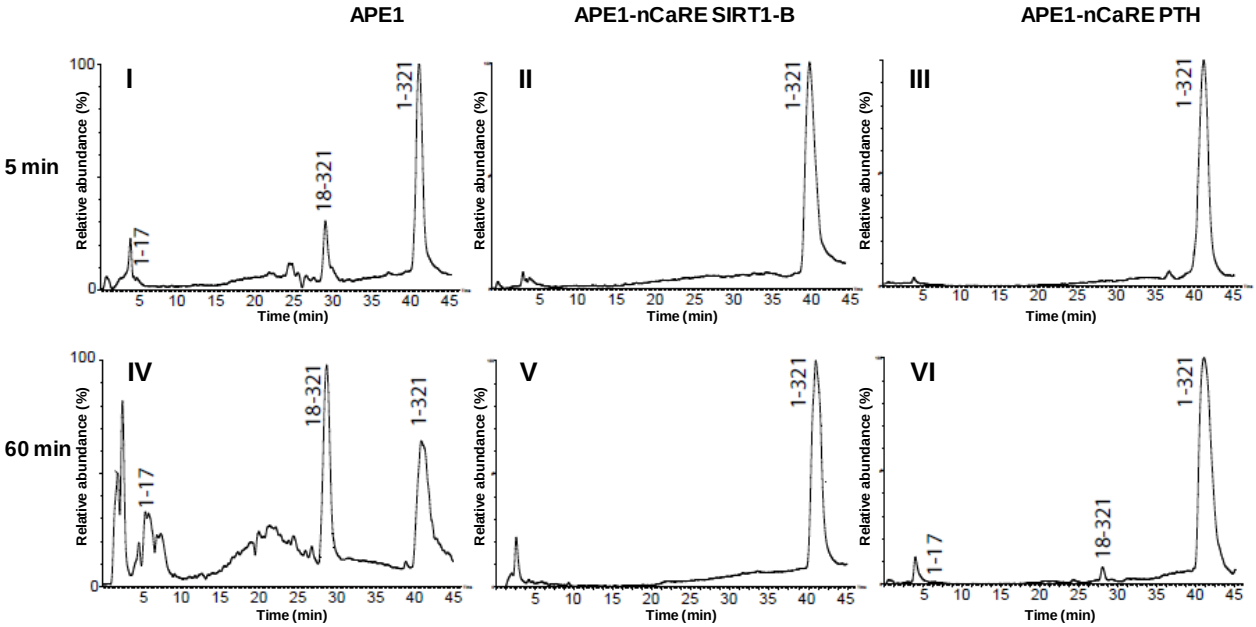

Supplemental Figure S6

A

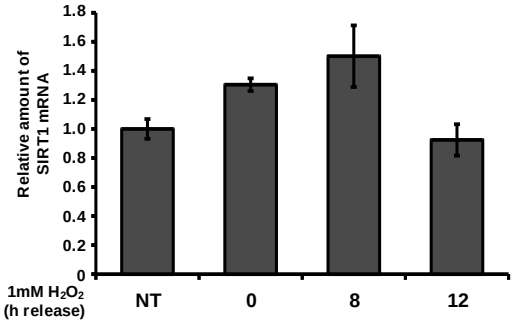

B

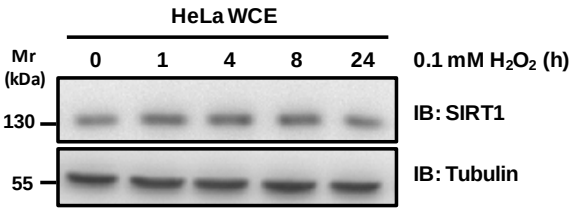

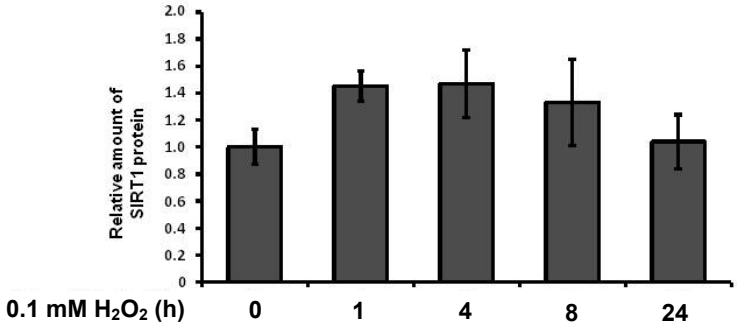

C

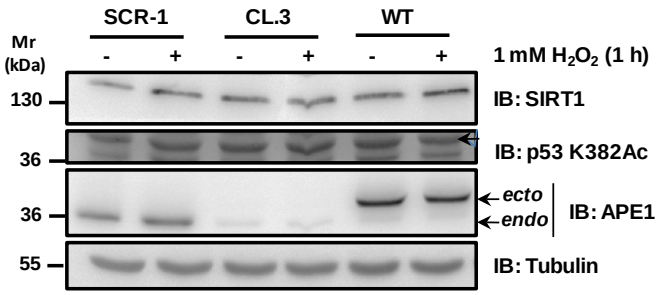

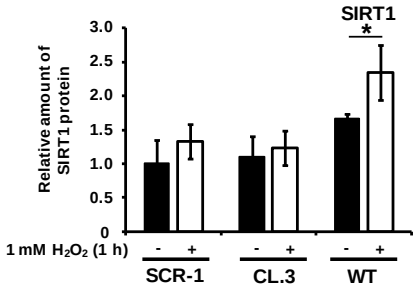

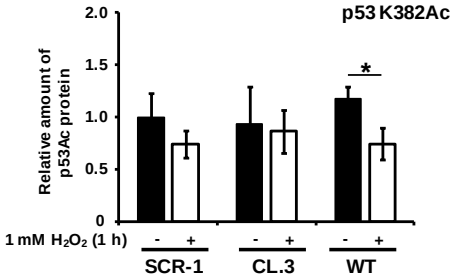

Supplemental Figure S7

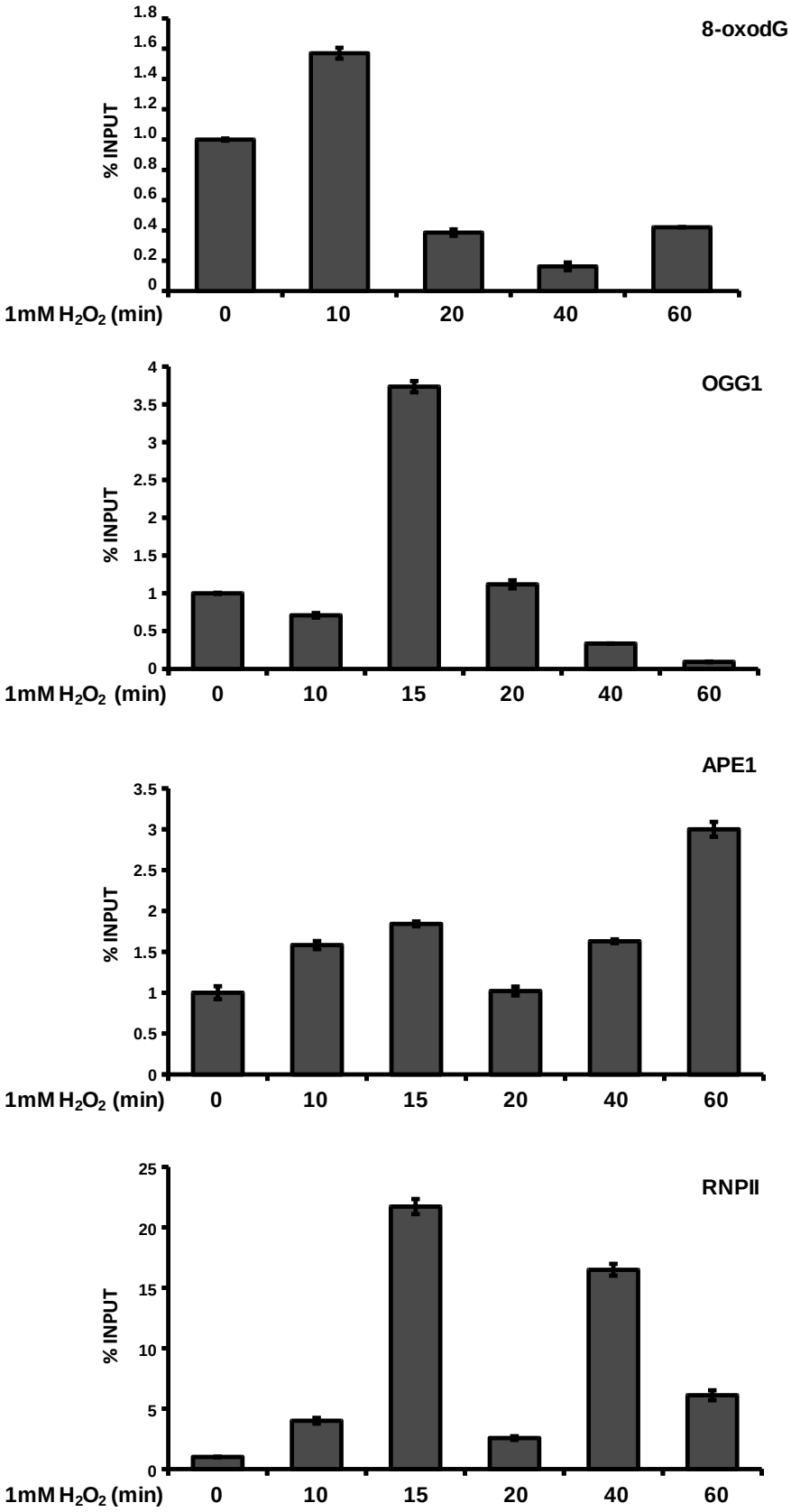

Supplemental Figure S8

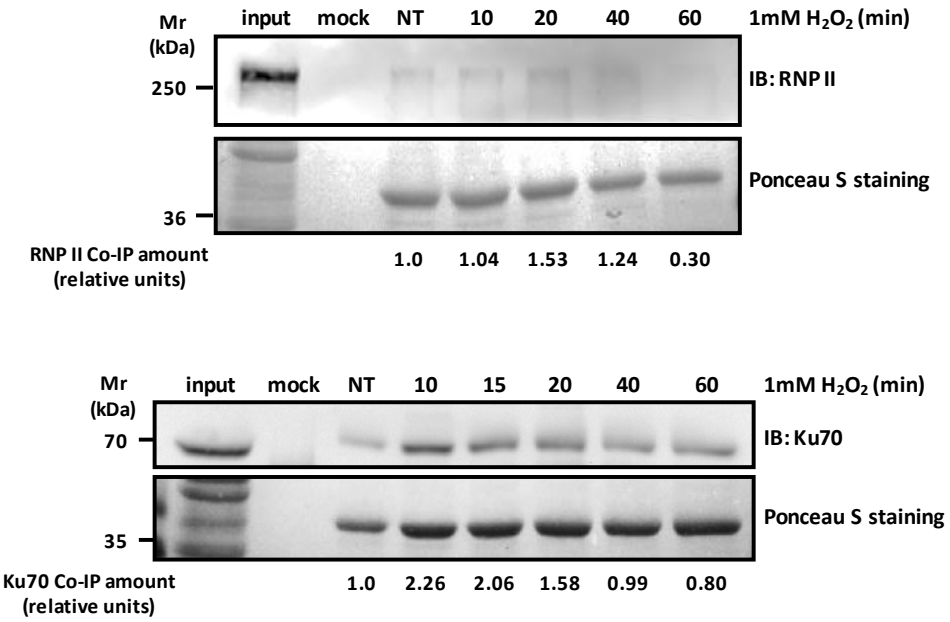

Supplemental Figure S9

A

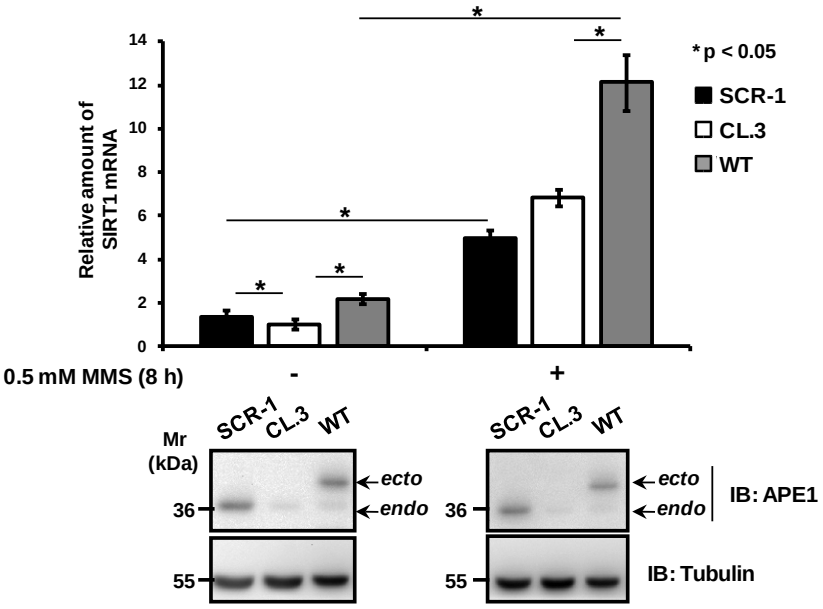

B

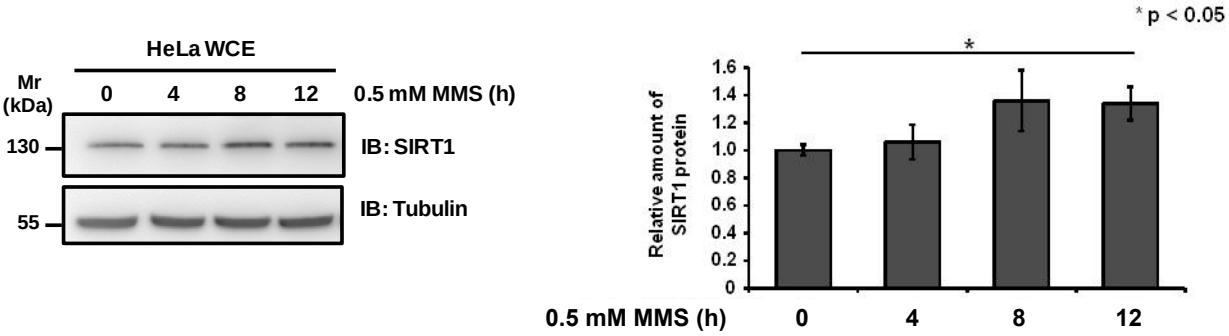

Supplemental Table 1

GO ID	n_annotation	n_both	expect	pv	-	
GO:0044424	10446	291	187.2580	8.69E-028	intracellular part	C
GO:0005622	10863	296	194.7340	7.22E-027	intracellular	C
GO:0043229	8870	260	159.0070	8.72E-026	intracellular organelle	C
GO:0043226	8885	260	159.2750	1.18E-025	organelle	C
GO:0005515	8150	238	146.1000	9.42E-022	protein binding	F
GO:0043231	7836	232	140.4710	1.03E-021	intracellular membrane-bounded organelle	C
GO:0043227	7845	232	140.6320	1.22E-021	membrane-bounded organelle	C
GO:0044464	14446	334	258.9640	4.67E-019	cell part	C
GO:0005623	14447	334	258.9820	4.74E-019	cell	C
GO:0005634	5052	168	90.5638	1.39E-018	nucleus	C
GO:0044446	3929	139	70.4326	5.42E-017	intracellular organelle part	C
GO:0044422	3957	139	70.9345	1.00E-016	organelle part	C
GO:0044428	1616	79	28.9690	1.56E-016	nuclear part	C
GO:0005737	7181	206	128.7290	2.43E-016	cytoplasm	C
GO:0005575	15609	344	279.8120	3.50E-016	cellular_component	C
GO:0006139	1842	82	33.0203	7.61E-015	nucleobase, nucleoside, nucleotide and nucleic acid metabolic process	P
GO:0009987	10893	267	195.2720	5.09E-014	cellular process	P
GO:0005488	12806	298	229.5650	6.67E-014	binding	F
GO:0006807	2248	90	40.2984	1.42E-013	nitrogen compound metabolic process	P
GO:0044260	3877	129	69.5004	1.61E-013	cellular macromolecule metabolic process	P
GO:0043232	2536	97	45.4612	1.91E-013	intracellular non-membrane-bounded organelle	C
GO:0043228	2536	97	45.4612	1.91E-013	non-membrane-bounded organelle	C
GO:0044237	5431	162	97.3579	2.93E-013	cellular metabolic process	P
GO:0031981	1231	60	22.0673	1.44E-012	nuclear lumen	C
GO:0016070	938	51	16.8149	1.57E-012	RNA metabolic process	P
GO:0008150	14455	319	259.1250	2.69E-012	biological_process	P
GO:0031974	1610	69	28.8614	9.32E-012	membrane-enclosed lumen	C
GO:0043233	1575	68	28.2340	9.77E-012	organelle lumen	C
GO:0070013	1539	67	27.5886	9.91E-012	intracellular organelle lumen	C
GO:0044238	5664	161	101.5350	2.39E-011	primary metabolic process	P
GO:0043170	4436	135	79.5212	2.73E-011	macromolecule metabolic process	P
GO:0043067	740	42	13.2655	4.62E-011	regulation of programmed cell death	P

GO:0010941	742	42	13.3013	5.02E-011	regulation of cell death	P
GO:0042981	731	41	13.1042	1.15E-010	regulation of apoptosis	P
GO:0003674	15294	327	274.1650	1.17E-010	molecular_function	F
GO:0032991	3223	106	57.7766	1.29E-010	macromolecular complex	C
GO:0008152	6464	173	115.8760	4.09E-010	metabolic process	P
GO:0005654	857	42	15.3629	3.91E-009	nucleoplasm	C
GO:0048519	1704	63	30.5465	2.85E-008	negative regulation of biological process	P
GO:0048523	1550	59	27.7858	3.06E-008	negative regulation of cellular process	P
GO:0005856	1386	54	24.8459	6.01E-008	cytoskeleton	C
GO:0006996	1386	54	24.8459	6.01E-008	organelle organization	P
GO:0044444	4724	129	84.6840	1.06E-007	cytoplasmic part	C
GO:0010467	1326	51	23.7703	2.18E-007	gene expression	P
GO:0044248	1081	44	19.3784	3.53E-007	cellular catabolic process	P
GO:0034645	1164	46	20.8663	4.30E-007	cellular macromolecule biosynthetic process	P
GO:0022402	542	28	9.7161	6.19E-007	cell cycle process	P
GO:0009059	1182	46	21.1889	6.59E-007	macromolecule biosynthetic process	P
GO:0044430	893	38	16.0082	8.12E-007	cytoskeletal part	C
GO:0044249	2001	66	35.8706	8.52E-007	cellular biosynthetic process	P
GO:0016043	2593	79	46.4830	1.37E-006	cellular component organization	P
GO:0044265	783	34	14.0363	2.04E-006	cellular macromolecule catabolic process	P
GO:0044267	2446	75	43.8478	2.15E-006	cellular protein metabolic process	P
GO:0016071	359	21	6.4356	2.39E-006	mRNA metabolic process	P
GO:0009058	2062	66	36.9641	2.40E-006	biosynthetic process	P
GO:0043234	2546	77	45.6404	2.55E-006	protein complex	C
GO:0034660	248	17	4.4457	2.70E-006	ncRNA metabolic process	P
GO:0005730	429	23	7.6904	3.44E-006	nucleolus	C
GO:0007010	439	23	7.8697	5.04E-006	cytoskeleton organization	P
GO:0006259	538	26	9.6444	5.27E-006	DNA metabolic process	P
GO:0006396	540	26	9.6802	5.63E-006	RNA processing	P
GO:0000278	352	20	6.3101	6.40E-006	mitotic cell cycle	P
GO:0006403	95	10	1.7030	7.96E-006	RNA localization	P
GO:0043065	360	20	6.4535	8.92E-006	positive regulation of apoptosis	P
GO:0042802	624	28	11.1860	9.19E-006	identical protein binding	F

GO:0043068	363	20	6.5073	1.01E-005	positive regulation of programmed cell death	P
GO:0016874	426	22	7.6366	1.01E-005	ligase activity	F
GO:0010942	365	20	6.5431	1.09E-005	positive regulation of cell death	P
GO:0007049	738	31	13.2296	1.13E-005	cell cycle	P
GO:0005200	83	9	1.4879	1.78E-005	structural constituent of cytoskeleton	F
GO:0015629	347	19	6.2204	1.83E-005	actin cytoskeleton	C
GO:0005916	10	4	0.1793	1.96E-005	fascia adherens	C
GO:0008092	516	24	9.2500	2.27E-005	cytoskeletal protein binding	F
GO:0015931	108	10	1.9360	2.48E-005	nucleobase, nucleoside, nucleotide and nucleic acid transport	P
GO:0003723	704	29	12.6201	3.11E-005	RNA binding	F
GO:0003779	330	18	5.9157	3.18E-005	actin binding	F
GO:0019538	2968	82	53.2054	3.42E-005	protein metabolic process	P
GO:0043038	70	8	1.2548	3.55E-005	amino acid activation	P
GO:0006418	70	8	1.2548	3.55E-005	tRNA aminoacylation for protein translation	P
GO:0043039	70	8	1.2548	3.55E-005	tRNA aminoacylation	P
GO:0044085	1133	40	20.3105	3.56E-005	cellular component biogenesis	P
GO:0022403	399	20	7.1526	3.90E-005	cell cycle phase	P
GO:0004812	71	8	1.2728	3.94E-005	aminoacyl-tRNA ligase activity	F
GO:0016876	71	8	1.2728	3.94E-005	ligase activity, forming aminoacyl-tRNA and related compounds	F
GO:0016875	71	8	1.2728	3.94E-005	ligase activity, forming carbon-oxygen bonds	F
GO:0051236	92	9	1.6492	4.08E-005	establishment of RNA localization	P
GO:0050657	92	9	1.6492	4.08E-005	nucleic acid transport	P
GO:0050658	92	9	1.6492	4.08E-005	RNA transport	P
GO:0000049	23	5	0.4123	4.65E-005	tRNA binding	F
GO:0006399	142	11	2.5455	5.22E-005	tRNA metabolic process	P
GO:0006950	2005	60	35.9423	5.46E-005	response to stress	P
GO:0043632	548	24	9.8236	5.90E-005	modification-dependent macromolecule catabolic process	P
GO:0019941	548	24	9.8236	5.90E-005	modification-dependent protein catabolic process	P
GO:0030529	550	24	9.8595	6.24E-005	ribonucleoprotein complex	C
GO:0006402	39	6	0.6991	6.31E-005	mRNA catabolic process	P
GO:0065009	933	34	16.7253	7.66E-005	regulation of molecular function	P
GO:0006261	58	7	1.0397	7.71E-005	DNA-dependent DNA replication	P
GO:0006401	59	7	1.0577	8.62E-005	RNA catabolic process	P

GO:0000184	26	5	0.4661	8.70E-005	nuclear-transcribed mRNA catabolic process, nonsense-mediated decay	P
GO:0006520	263	15	4.7146	8.76E-005	cellular amino acid metabolic process	P
GO:0005625	325	17	5.8261	8.79E-005	soluble fraction	C
GO:0015630	527	23	9.4472	8.84E-005	microtubule cytoskeleton	C
GO:0005829	1141	39	20.4539	8.93E-005	cytosol	C
GO:0007067	205	13	3.6749	8.95E-005	mitosis	P
GO:0000280	205	13	3.6749	8.95E-005	nuclear division	P

Supplemental Table 2

Ensembl ID	Gene title	Gene symbol	Chr. location
ENSG00000090861	alanyl-tRNA synthetase	AARS	chr16q22
ENSG00000100823	APEX nuclease (multifunctional DNA repair enzyme) 1	APEX1	chr14q11.2-q12
ENSG00000062725	amyloid beta precursor protein (cytoplasmic tail) binding protein 2	APPBP2	chr17q21-q23
ENSG00000162704	actin related protein 2/3 complex, subunit 5, 16kDa	ARPC5	chr1q25.3
ENSG00000113732	ATPase, H+ transporting, lysosomal 9kDa, V0 subunit e	ATP6V0E	chr5q35.1
ENSG00000156735	BCL2-associated athanogene 4	BAG4	chr8p12
ENSG00000060762	brain protein 44-like	BRP44L	chr6q27
ENSG00000130303	bone marrow stromal cell antigen 2	BST2	chr19p13.2
ENSG00000164941	chromosome 8 open reading frame 52	C8orf52	chr8q22.1
ENSG00000110619	cysteinyl-tRNA synthetase	CARS	chr11p15.5
ENSG00000160200	cystathionine-beta-synthase	CBS	chr21q22.3
ENSG00000117877	CD3E antigen, epsilon polypeptide associated protein	CD3EAP	chr19q13.3
ENSG00000010278	CD9 antigen (p24)	CD9	chr12p13.3
ENSG00000153774	craniofacial development protein 1	CFDP1	chr16q22.2-q22.3
ENSG00000149600	COMM domain containing 7	COMMD7	chr20q11.21
ENSG00000175215	CTD (carboxy-terminal domain, RNA polymerase II, polypeptide A) small phosphatase 2	CTDSP2	chr12q13-q15

ENSG00000143079	CTTNBP2 N-terminal like	CTTNBP2NL	chr1p13.2
ENSG00000108406	DEAH (Asp-Glu-Ala-His) box polypeptide 40	DHX40	chr17q23.2
ENSG00000120738	Early growth response 1	EGR1	chr5q31.1
ENSG00000147677	eukaryotic translation initiation factor 3, subunit 3 gamma, 40kDa	EIF3S3	chr8q24.11
ENSG00000187840	eukaryotic translation initiation factor 4E binding protein 1	EIF4EBP1	chr8p12
ENSG00000136628	glutamyl-prolyl-tRNA synthetase	EPRS	chr1q41-q42
ENSG00000147874	family with sequence similarity 29, member A	FAM29A	chr9p22.1
ENSG00000104872	hypothetical protein FLJ20643	FLJ20643	chr19q13.33
ENSG00000143575	HCLS1 associated protein X-1	HAX1	chr1q21.3
ENSG00000185359	hepatocyte growth factor-regulated tyrosine kinase substrate	HGS	chr17q25
ENSG00000189159	hematological and neurological expressed 1	HN1	chr17q25.1
ENSG00000131373	2-hydroxyphytanoyl-CoA lyase	HPCL2	chr3p25.1
ENSG00000166411	isocitrate dehydrogenase 3 (NAD+) alpha	IDH3A	chr15q25.1-q25.2
ENSG00000130522	jun D proto-oncogene	JUND	chr19p13.2
ENSG00000145725	KIAA0433 protein	KIAA0433	chr5q21.1
ENSG00000052749	KIAA0690	KIAA0690	chr10q24.1
ENSG00000112200	KIAA1702 protein	KIAA1702	chr6p11

ENSG00000118193	kinesin family member 14	KIF14	chr1pter-q31.3
ENSG00000109790	kelch-like 5 (Drosophila)	KLHL5	chr4p14
ENSG00000126214	kinesin 2	KNS2	chr14q32.3
ENSG00000130164	low density lipoprotein receptor (familial hypercholesterolemia)	LDLR	chr19p13.3
ENSG00000133895	multiple endocrine neoplasia I	MEN1	chr11q13
ENSG00000109919	mitochondrial carrier homolog 2 (C. elegans)	MTCH2	chr11p11.2
ENSG00000102908	nuclear factor of activated T-cells 5, tonicity-responsive	NFAT5	chr16q22.1
ENSG00000171246	neuronal pentraxin I	NPTX1	chr17q25.1-q25.2
ENSG00000135318	5'-nucleotidase, ecto (CD73)	NT5E	chr6q14-q21
ENSG00000025293	PHD finger protein 20	PHF20	chr20q11.22-q11.23
ENSG00000149547	translokin	PIG8	chr11q21
ENSG00000198056	primase, polypeptide 1, 49kDa	PRIM1	chr12q13
ENSG00000034677	ring finger protein 19	RNF19	chr8q22
ENSG00000096717	sirtuin (silent mating type information regulation 2 homolog) 1 (S. cerevisiae)	SIRT1	chr10q21.3
ENSG00000105281	solute carrier family 1 (neutral amino acid transporter), member 5	SLC1A5	chr19q13.3
ENSG00000127616	SWI/SNF related, matrix associated, actin dependent regulator of chromatin, subfamily a, member 4	SMARCA4	chr19p13.2
ENSG00000163029	SMC6 structural maintenance of chromosomes 6-like 1 (yeast)	SMC6L1	chr2p24.2

ENSG00000197694	spectrin, alpha, non-erythrocytic 1 (alpha-fodrin)	SPTAN1	chr9q33-q34
ENSG00000173465	Sjogren's syndrome/scleroderma autoantigen 1	SSSCA1	chr11q13.1
ENSG00000144043	testis expressed sequence 261	TEX261	chr2p13.3
ENSG00000035862	TIMP metallopeptidase inhibitor 2	TIMP2	chr17q25
ENSG00000198211	tubulin, beta 3	TUBB3	chr16q24.3
ENSG00000165280	valosin-containing protein	VCP	chr9p13.3
ENSG00000134684	tyrosyl-tRNA synthetase	YARS	chr1p35.1

Supplemental Table 3

GO term ID	Annotations	# of annotated genes in the input list (Total # of genes in the input list)	# of annotated genes in the reference list (Total # of genes in the reference list)	Hypergeometric Distribution (Fisher's exact test)	Corrected Hypergeometric Dist. (Fisher's exact test)	Genes
GO:0010467	gene expression (BP)	6(57)	408(34208)	6,02E-05	9,97E-03	EIF4EBP1 , YARS, AARS, EPRS, CARS, EIF3H
GO:0045944	positive regulation of transcription from RNA polymerase II promoter (BP)	6(57)	578(34208)	3,96E-04	1,87E-02	SIRT1 , EGR1, JUND, SMARCA4, MEN1, NFAT5
GO:0006281	DNA repair (BP)	5(57)	285(34208)	1,14E-04	1,26E-02	SIRT1, SMC6, VCP, MEN1, APEX1
GO:0006810	transport (BP)	5(57)	604(34208)	3,32E-03	2,89E-02	VCP, LDLR, NPTX1, ATP6V0E1, MTCH2
GO:0006418	tRNA aminoacylation for protein translation (BP)	4(57)	43(34208)	8,14E-07	2,70E-04	YARS, AARS, EPRS, CARS
GO:0008285	negative regulation of cell proliferation (BP)	4(57)	341(34208)	2,53E-03	2,46E-02	HGS , MEN1, CD9, TIMP2
GO:0045892	negative regulation of transcription, DNA-dependent (BP)	4(57)	401(34208)	4,50E-03	2,37E-02	SIRT1 , SMARCA4, MEN1, COMMD7
GO:0000122	negative regulation of transcription from RNA polymerase II promoter (BP)	4(57)	416(34208)	5,13E-03	2,23E-02	SIRT1, EGR1, SMARCA4, MEN1
GO:0007018	microtubule-based movement (BP)	3(57)	90(34208)	4,65E-04	1,92E-02	KLC1, KIF14, TUBB3
GO:0030308	negative regulation of cell growth (BP)	3(57)	113(34208)	9,02E-04	2,71E-02	SIRT1, SMARCA4, EI24
GO:0006974	response to DNA damage stimulus (BP)	3(57)	129(34208)	1,32E-03	3,12E-02	SIRT1, VCP, MEN1
GO:0043065	positive regulation of apoptotic process (BP)	3(57)	178(34208)	3,30E-03	3,03E-02	TEX261, SIRT1, MEN1
GO:0006457	protein folding (BP)	3(57)	182(34208)	3,51E-03	1,94E-02	AARS, BAG4, TUBB3
GO:0044267	cellular protein metabolic process (BP)	3(57)	284(34208)	1,19E-02	3,40E-02	EIF4EBP1, TUBB3, EIF3H
GO:0060766	negative regulation of androgen receptor signaling pathway (BP)	2(57)	10(34208)	1,22E-04	1,01E-02	SIRT1, SMARCA4

GO:0060135	maternal process involved in female pregnancy (BP)	2(57)	14(34208)	2,45E-04	1,62E-02	MEN1, CBS
GO:0002076	osteoblast development (BP)	2(57)	16(34208)	3,22E-04	1,78E-02	JUND, MEN1
GO:0045739	positive regulation of DNA repair (BP)	2(57)	23(34208)	6,75E-04	2,48E-02	SIRT1, APEX1
GO:0030968	endoplasmic reticulum unfolded protein response (BP)	2(57)	25(34208)	7,98E-04	2,64E-02	VCP, AARS
GO:0043280	positive regulation of cysteine-type endopeptidase activity involved in apoptotic process (BP)	2(57)	27(34208)	9,32E-04	2,57E-02	SIRT1, MEN1
GO:0071356	cellular response to tumor necrosis factor (BP)	2(57)	28(34208)	1,00E-03	2,55E-02	SIRT1, BAG4
GO:0045768	positive regulation of anti-apoptosis (BP)	2(57)	41(34208)	2,15E-03	2,22E-02	SIRT1, APEX1
GO:0045669	positive regulation of osteoblast differentiation (BP)	2(57)	42(34208)	2,25E-03	2,26E-02	JUND, MEN1
GO:0032088	negative regulation of NF-kappaB transcription factor activity (BP)	2(57)	46(34208)	2,69E-03	2,55E-02	SIRT1, COMMD7
GO:0042632	cholesterol homeostasis (BP)	2(57)	51(34208)	3,30E-03	2,95E-02	SIRT1, LDLR
GO:0043161	proteasomal ubiquitin-dependent protein catabolic process (BP)	2(57)	52(34208)	3,43E-03	1,92E-02	SIRT1, VCP
GO:0043433	negative regulation of sequence-specific DNA binding transcription factor activity (BP)	2(57)	54(34208)	3,69E-03	1,97E-02	SIRT1, MEN1
GO:0006338	chromatin remodeling (BP)	2(57)	54(34208)	3,69E-03	1,97E-02	SMARCA4, MEN1
GO:0032868	response to insulin stimulus (BP)	2(57)	62(34208)	4,84E-03	2,50E-02	SIRT1, EGR1
GO:0006310	DNA recombination (BP)	2(57)	86(34208)	9,12E-03	3,05E-02	SMC6, APEX1
GO:0006928	cellular component movement (BP)	2(57)	95(34208)	1,10E-02	3,35E-02	CD9, ARPC5
GO:0042127	regulation of cell proliferation (BP)	2(57)	101(34208)	1,24E-02	3,51E-02	SIRT1, CFDP1
GO:0008286	insulin receptor signaling pathway (BP)	2(57)	139(34208)	2,26E-02	4,89E-02	EIF4EBP1, ATP6V0E1

GO:0043418	homocysteine catabolic process (BP)	1(57)	1(34208)	1,67E-03	1,78E-02	CBS
GO:0019343	cysteine biosynthetic process via cystathionine (BP)	1(57)	1(34208)	1,67E-03	1,78E-02	CBS
GO:0019346	transsulfuration (BP)	1(57)	1(34208)	1,67E-03	1,78E-02	CBS
GO:0006535	cysteine biosynthetic process from serine (BP)	1(57)	1(34208)	1,67E-03	1,78E-02	CBS
GO:0006437	tyrosyl-tRNA aminoacylation (BP)	1(57)	1(34208)	1,67E-03	1,78E-02	YARS
GO:0031062	positive regulation of histone methylation (BP)	1(57)	1(34208)	1,67E-03	1,78E-02	MEN1
GO:0046086	adenosine biosynthetic process (BP)	1(57)	1(34208)	1,67E-03	1,78E-02	NT5E
GO:0072303	positive regulation of glomerular metanephric mesangial cell proliferation (BP)	1(57)	1(34208)	1,67E-03	1,78E-02	EGR1
GO:0072110	glomerular mesangial cell proliferation (BP)	1(57)	1(34208)	1,67E-03	1,78E-02	EGR1
GO:0033233	regulation of protein sumoylation (BP)	1(57)	1(34208)	1,67E-03	1,78E-02	EGR1
GO:2000655	negative regulation of cellular response to testosterone stimulus (BP)	1(57)	1(34208)	1,67E-03	1,78E-02	SIRT1
GO:2000480	negative regulation of cAMP-dependent protein kinase activity (BP)	1(57)	1(34208)	1,67E-03	1,78E-02	SIRT1
GO:0006343	establishment of chromatin silencing (BP)	1(57)	1(34208)	1,67E-03	1,78E-02	SIRT1
GO:2000757	negative regulation of peptidyl-lysine acetylation (BP)	1(57)	1(34208)	1,67E-03	1,78E-02	SIRT1
GO:0034391	regulation of smooth muscle cell apoptosis (BP)	1(57)	1(34208)	1,67E-03	1,78E-02	SIRT1
GO:0031937	positive regulation of chromatin silencing (BP)	1(57)	1(34208)	1,67E-03	1,78E-02	SIRT1
GO:0031393	negative regulation of prostaglandin biosynthetic process (BP)	1(57)	1(34208)	1,67E-03	1,78E-02	SIRT1
GO:0060385	axonogenesis involved in innervation (BP)	1(57)	2(34208)	3,33E-03	1,90E-02	NPTX1

GO:2000481	positive regulation of cAMP-dependent protein kinase activity (BP)	1(57)	2(34208)	3,33E-03	1,90E-02	SIRT1
GO:2000773	negative regulation of cellular senescence (BP)	1(57)	2(34208)	3,33E-03	1,90E-02	SIRT1
GO:0035617	stress granule disassembly (BP)	1(57)	2(34208)	3,33E-03	1,90E-02	KLC1
GO:0006424	glutamyl-tRNA aminoacylation (BP)	1(57)	2(34208)	3,33E-03	1,90E-02	EPRS
GO:0016239	positive regulation of macroautophagy (BP)	1(57)	2(34208)	3,33E-03	1,90E-02	SIRT1
GO:0006433	prolyl-tRNA aminoacylation (BP)	1(57)	2(34208)	3,33E-03	1,90E-02	EPRS
GO:0006423	cysteinyl-tRNA aminoacylation (BP)	1(57)	2(34208)	3,33E-03	1,90E-02	CARS
GO:0043506	regulation of JUN kinase activity (BP)	1(57)	2(34208)	3,33E-03	1,90E-02	CBS
GO:0030823	regulation of cGMP metabolic process (BP)	1(57)	2(34208)	3,33E-03	1,90E-02	CBS
GO:0070814	hydrogen sulfide biosynthetic process (BP)	1(57)	2(34208)	3,33E-03	1,90E-02	CBS
GO:0019448	L-cysteine catabolic process (BP)	1(57)	2(34208)	3,33E-03	1,90E-02	CBS
GO:0010899	regulation of phosphatidylcholine catabolic process (BP)	1(57)	2(34208)	3,33E-03	1,90E-02	LDLR
GO:0018394	peptidyl-lysine acetylation (BP)	1(57)	2(34208)	3,33E-03	1,90E-02	SIRT1
GO:0080134	regulation of response to stress (BP)	1(57)	2(34208)	3,33E-03	1,90E-02	SIRT1
GO:0002051	osteoblast fate commitment (BP)	1(57)	2(34208)	3,33E-03	1,90E-02	MEN1
GO:0006196	AMP catabolic process (BP)	1(57)	2(34208)	3,33E-03	1,90E-02	NT5E
GO:0000720	pyrimidine dimer repair by nucleotide-excision repair (BP)	1(57)	2(34208)	3,33E-03	1,90E-02	SIRT1
GO:0071506	cellular response to mycophenolic acid (BP)	1(57)	2(34208)	3,33E-03	1,90E-02	EGR1

GO:0032071	regulation of endodeoxyribonuclease activity (BP)	1(57)	2(34208)	3,33E-03	1,90E-02	SIRT1
GO:0000492	box C/D snoRNP assembly (BP)	1(57)	3(34208)	4,99E-03	2,20E-02	PIH1D1
GO:0006565	L-serine catabolic process (BP)	1(57)	3(34208)	4,99E-03	2,20E-02	CBS
GO:0051097	negative regulation of helicase activity (BP)	1(57)	3(34208)	4,99E-03	2,20E-02	SIRT1
GO:0009166	nucleotide catabolic process (BP)	1(57)	3(34208)	4,99E-03	2,20E-02	NT5E
GO:0002821	positive regulation of adaptive immune response (BP)	1(57)	3(34208)	4,99E-03	2,20E-02	SIRT1
GO:0001776	leukocyte homeostasis (BP)	1(57)	3(34208)	4,99E-03	2,20E-02	MEN1
GO:0070508	cholesterol import (BP)	1(57)	3(34208)	4,99E-03	2,20E-02	LDLR
GO:0035356	cellular triglyceride homeostasis (BP)	1(57)	3(34208)	4,99E-03	2,20E-02	SIRT1
GO:0006419	alanyl-tRNA aminoacylation (BP)	1(57)	3(34208)	4,99E-03	2,20E-02	AARS
GO:0009414	response to water deprivation (BP)	1(57)	3(34208)	4,99E-03	2,20E-02	CD9
GO:0006344	maintenance of chromatin silencing (BP)	1(57)	3(34208)	4,99E-03	2,20E-02	SIRT1
GO:2000111	positive regulation of macrophage apoptosis (BP)	1(57)	4(34208)	6,65E-03	2,45E-02	SIRT1
GO:0006269	DNA replication, synthesis of RNA primer (BP)	1(57)	4(34208)	6,65E-03	2,45E-02	PRIM1
GO:0010906	regulation of glucose metabolic process (BP)	1(57)	4(34208)	6,65E-03	2,45E-02	SIRT1
GO:2000774	positive regulation of cellular senescence (BP)	1(57)	4(34208)	6,65E-03	2,45E-02	SIRT1
GO:0030814	regulation of cAMP metabolic process (BP)	1(57)	4(34208)	6,65E-03	2,45E-02	TIMP2
GO:0007035	vacuolar acidification (BP)	1(57)	4(34208)	6,65E-03	2,45E-02	ATP6V0E1

GO:0006020	inositol metabolic process (BP)	1(57)	4(34208)	6,65E-03	2,45E-02	PPIP5K2
GO:0070842	aggresome assembly (BP)	1(57)	4(34208)	6,65E-03	2,45E-02	VCP
GO:0034983	peptidyl-lysine deacetylation (BP)	1(57)	4(34208)	6,65E-03	2,45E-02	SIRT1
GO:0006868	glutamine transport (BP)	1(57)	4(34208)	6,65E-03	2,45E-02	SLC1A5
GO:0050667	homocysteine metabolic process (BP)	1(57)	4(34208)	6,65E-03	2,45E-02	CBS
GO:0070857	regulation of bile acid biosynthetic process (BP)	1(57)	4(34208)	6,65E-03	2,45E-02	SIRT1
GO:0070932	histone H3 deacetylation (BP)	1(57)	4(34208)	6,65E-03	2,45E-02	SIRT1
GO:0033158	regulation of protein import into nucleus, translocation (BP)	1(57)	4(34208)	6,65E-03	2,45E-02	SIRT1
GO:0006346	methylation-dependent chromatin silencing (BP)	1(57)	5(34208)	8,30E-03	2,80E-02	SIRT1
GO:0030913	paranodal junction assembly (BP)	1(57)	5(34208)	8,30E-03	2,80E-02	CD9
GO:0006563	L-serine metabolic process (BP)	1(57)	5(34208)	8,30E-03	2,80E-02	CBS
GO:0001678	cellular glucose homeostasis (BP)	1(57)	5(34208)	8,30E-03	2,80E-02	SIRT1
GO:0071504	cellular response to heparin (BP)	1(57)	5(34208)	8,30E-03	2,80E-02	EGR1
GO:0030970	retrograde protein transport, ER to cytosol (BP)	1(57)	5(34208)	8,30E-03	2,80E-02	VCP
GO:0043039	tRNA aminoacylation (BP)	1(57)	5(34208)	8,30E-03	2,80E-02	AARS
GO:0032925	regulation of activin receptor signaling pathway (BP)	1(57)	5(34208)	8,30E-03	2,80E-02	MEN1
GO:0008088	axon cargo transport (BP)	1(57)	6(34208)	9,96E-03	3,05E-02	KLC1
GO:0046628	positive regulation of insulin receptor signaling pathway (BP)	1(57)	6(34208)	9,96E-03	3,05E-02	SIRT1

GO:0021587	cerebellum morphogenesis (BP)	1(57)	6(34208)	9,96E-03	3,05E-02	CBS
GO:0003407	neural retina development (BP)	1(57)	6(34208)	9,96E-03	3,05E-02	SMARCA4
GO:0001561	fatty acid alpha-oxidation (BP)	1(57)	6(34208)	9,96E-03	3,05E-02	HACL1
GO:0046426	negative regulation of JAK-STAT cascade (BP)	1(57)	6(34208)	9,96E-03	3,05E-02	HGS
GO:0006642	triglyceride mobilization (BP)	1(57)	6(34208)	9,96E-03	3,05E-02	SIRT1
GO:0046621	negative regulation of organ growth (BP)	1(57)	6(34208)	9,96E-03	3,05E-02	MEN1
GO:0006102	isocitrate metabolic process (BP)	1(57)	6(34208)	9,96E-03	3,05E-02	IDH3A
GO:0071480	cellular response to gamma radiation (BP)	1(57)	7(34208)	1,16E-02	3,34E-02	EGR1
GO:0010867	positive regulation of triglyceride biosynthetic process (BP)	1(57)	7(34208)	1,16E-02	3,34E-02	LDLR
GO:0051974	negative regulation of telomerase activity (BP)	1(57)	7(34208)	1,16E-02	3,34E-02	MEN1
GO:0000183	chromatin silencing at rDNA (BP)	1(57)	7(34208)	1,16E-02	3,34E-02	SIRT1
GO:0060351	cartilage development involved in endochondral bone morphogenesis (BP)	1(57)	7(34208)	1,16E-02	3,34E-02	CBS
GO:0006734	NADH metabolic process (BP)	1(57)	7(34208)	1,16E-02	3,34E-02	IDH3A
GO:0031929	TOR signaling cascade (BP)	1(57)	8(34208)	1,33E-02	3,48E-02	EIF4EBP1
GO:0006835	dicarboxylic acid transport (BP)	1(57)	8(34208)	1,33E-02	3,48E-02	SLC1A5
GO:0000012	single strand break repair (BP)	1(57)	8(34208)	1,33E-02	3,48E-02	SIRT1
GO:0055089	fatty acid homeostasis (BP)	1(57)	8(34208)	1,33E-02	3,48E-02	SIRT1
GO:0034383	low-density lipoprotein particle clearance (BP)	1(57)	8(34208)	1,33E-02	3,48E-02	LDLR

GO:0006400	tRNA modification (BP)	1(57)	8(34208)	1,33E-02	3,48E-02	AARS
GO:0030299	intestinal cholesterol absorption (BP)	1(57)	8(34208)	1,33E-02	3,48E-02	LDLR
GO:0045348	positive regulation of MHC class II biosynthetic process (BP)	1(57)	8(34208)	1,33E-02	3,48E-02	SIRT1
GO:0006342	chromatin silencing (BP)	1(57)	8(34208)	1,33E-02	3,48E-02	SIRT1
GO:0021680	cerebellar Purkinje cell layer development (BP)	1(57)	9(34208)	1,49E-02	3,68E-02	AARS
GO:0015804	neutral amino acid transport (BP)	1(57)	9(34208)	1,49E-02	3,68E-02	SLC1A5
GO:0007342	fusion of sperm to egg plasma membrane (BP)	1(57)	9(34208)	1,49E-02	3,68E-02	CD9
GO:0001542	ovulation from ovarian follicle (BP)	1(57)	9(34208)	1,49E-02	3,68E-02	SIRT1
GO:0070498	interleukin-1-mediated signaling pathway (BP)	1(57)	9(34208)	1,49E-02	3,68E-02	EGR1
GO:0051593	response to folic acid (BP)	1(57)	9(34208)	1,49E-02	3,68E-02	CBS
GO:0031333	negative regulation of protein complex assembly (BP)	1(57)	9(34208)	1,49E-02	3,68E-02	EIF4EBP1
GO:0045749	negative regulation of S phase of mitotic cell cycle (BP)	1(57)	9(34208)	1,49E-02	3,68E-02	SMARCA4
GO:0000731	DNA synthesis involved in DNA repair (BP)	1(57)	10(34208)	1,65E-02	3,97E-02	SIRT1
GO:0034968	histone lysine methylation (BP)	1(57)	10(34208)	1,65E-02	3,97E-02	MEN1
GO:0043923	positive regulation by host of viral transcription (BP)	1(57)	10(34208)	1,65E-02	3,97E-02	SMARCA4
GO:0043518	negative regulation of DNA damage response, signal transduction by p53 class mediator (BP)	1(57)	10(34208)	1,65E-02	3,97E-02	SIRT1
GO:0006195	purine nucleotide catabolic process (BP)	1(57)	11(34208)	1,82E-02	4,15E-02	NT5E
GO:0045947	negative regulation of translational initiation (BP)	1(57)	11(34208)	1,82E-02	4,15E-02	EIF4EBP1

GO:0043488	regulation of mRNA stability (BP)	1(57)	11(34208)	1,82E-02	4,15E-02	APEX1
GO:0010875	positive regulation of cholesterol efflux (BP)	1(57)	11(34208)	1,82E-02	4,15E-02	SIRT1
GO:0043408	regulation of MAPK cascade (BP)	1(57)	11(34208)	1,82E-02	4,15E-02	TIMP2
GO:0031334	positive regulation of protein complex assembly (BP)	1(57)	11(34208)	1,82E-02	4,15E-02	VCP
GO:0006476	protein deacetylation (BP)	1(57)	11(34208)	1,82E-02	4,15E-02	SIRT1
GO:0016180	snRNA processing (BP)	1(57)	12(34208)	1,98E-02	4,37E-02	INTS8
GO:0050872	white fat cell differentiation (BP)	1(57)	12(34208)	1,98E-02	4,37E-02	SIRT1
GO:0080111	DNA demethylation (BP)	1(57)	12(34208)	1,98E-02	4,37E-02	APEX1
GO:0032007	negative regulation of TOR signaling cascade (BP)	1(57)	12(34208)	1,98E-02	4,37E-02	SIRT1
GO:0046135	pyrimidine nucleoside catabolic process (BP)	1(57)	12(34208)	1,98E-02	4,37E-02	NT5E
GO:0030301	cholesterol transport (BP)	1(57)	13(34208)	2,15E-02	4,67E-02	LDLR
GO:0030833	regulation of actin filament polymerization (BP)	1(57)	13(34208)	2,15E-02	4,67E-02	ARPC5
GO:0042176	regulation of protein catabolic process (BP)	1(57)	14(34208)	2,31E-02	4,90E-02	HGS
GO:0009303	rRNA transcription (BP)	1(57)	14(34208)	2,31E-02	4,90E-02	CD3EAP
GO:0050880	regulation of blood vessel size (BP)	1(57)	14(34208)	2,31E-02	4,90E-02	CBS

Supplemental Table 4

				APE1	APE1-SIRT1 nCaRE complex	APE1-PTH nCaRE complex	
Enzyme	**Time (min)**	**Peptide**	**Theoretical mass**	**Experimental mass**	**Experimental mass**	**Experimental mass**	**Primary cleavage site**
Trypsin/APE1 1:5000 (w/w)	**5**	**1-9**	1041.62_{mi}	1041.60_{mi}			K9 (K6)
		1-10	1169.72_{mi}	1169.68_{mi}			K10 (K7)
		10-321	34856.56_{av}	34854.12_{av}			K9 (K6)
		11-321	34727.40_{av}	34726.80_{av}			K10 (K7)
		1-321	35880.86_{av}	35879.87_{av}	35879.5_{av}	35880.22_{av}	
	15	**1-9**	1041.62_{mi}	1041.58_{mi}			K9 (K6)
		1-10	1169.72_{mi}	1169.67_{mi}			K10 (K7)
		10-321	34856.56_{av}	34856.70_{av}			K9 (K6)
		11-321	34727.40_{av}	34726.50_{av}			K10 (K7)
		11-27	1785.84_{mi}	1785.81_{mi}			
		11-30	2129.06_{mi}	2128.96_{mi}			
		31-321	32615.10_{av}	32613.80_{av}			
		1-321	35880.86_{av}	35879.46_{av}	35879.9_{av}	35879.95_{av}	

	30	**1-9**	1041.62 $_{mi}$	1041.59 $_{mi}$			K9 (K6)
		1-10	1169.72 $_{mi}$	1169.70 $_{mi}$			K10 (K7)
		10-321	34856.56$_{av}$	34858.76 $_{av}$			K9 (K6)
		11-321	34727.40$_{av}$	34726.72 $_{av}$			K10 (K7)
		11-27	1785.84 $_{mi}$	1785.82 $_{mi}$			
		11-30	2129.06 $_{mi}$	2128.03 $_{mi}$			
		31-321	32615.10$_{av}$	32613.75 $_{av}$			
		1-321	35880.86$_{av}$	35879.92 $_{av}$	35879.50 $_{av}$	35880.02 $_{av}$	
	60	**1-9**	1041.62 $_{mi}$	1041.57 $_{mi}$	1041.58 $_{mi}$	1041.60 $_{mi}$	K9 (K6)
		1-10	1169.72 $_{mi}$	1169.65 $_{mi}$			K10 (K7)
		10-321	34856.56 $_{av}$	34858.83 $_{av}$	34857.66 $_{av}$	34858.23 $_{av}$	K9 (K6)
		11-321	34727.40$_{av}$	34726.51 $_{av}$			K10 (K7)
		11-27	1785.84$_{mi}$	1785.79 $_{mi}$	1785.80 $_{mi}$	1785.80 $_{mi}$	
		11-30	2129.06$_{mi}$	2128.95 $_{mi}$		2129.10 $_{mi}$	
		31-321	32615.1$_{av}$	32613.28 $_{av}$	32614.13 $_{av}$	32614.58 $_{av}$	
		1-321	35880.86$_{av}$		35879.70 $_{av}$	35879.30 $_{av}$	

Endoprotease AspN/APE1 1:500 (w/w)		**1-17**	1768.97 $_{mi}$	1768.95 $_{mi}$			D18 (D15)
	5	**18-321**	34128.79 $_{av}$	34127.5 $_{av}$			D18 (D15)
		1-321	35880.96 $_{av}$	35878.6 $_{av}$	35879.10 $_{av}$	35877.50 $_{av}$	
		1-17	1768.97 $_{mi}$				D18 (D15)
	15	**18-321**	34128.79 $_{av}$	34127.4 $_{av}$			D18 (D15)
		1-321	35880.96 $_{av}$	35878.9 $_{av}$	35878.40 $_{av}$	35879.20 $_{av}$	
		1-17	1768.97 $_{mi}$	1768.96 $_{mi}$			D18 (D15)
	30	**18-321**	34128.79 $_{av}$	34126.9 $_{av}$			D18 (D15)
		1-321	35880.96 $_{av}$	35878.6 $_{av}$	35878.90 $_{av}$	35878.10 $_{av}$	
		1-17	1768.97 $_{mi}$	1798.94 $_{mi}$		1798.95 $_{mi}$	D18 (D15)
	60	**18-321**	34128.79 $_{av}$	34127.9 $_{av}$		34126.20 $_{av}$	D18 (D15)
		1-321	35880.96 $_{av}$	35879.02 $_{av}$	35875.60 $_{av}$	35877.70 $_{av}$	
Chimotrypsin/APE1 1:1000 (w/w)		**1-114**	12501.23 $_{av}$	12501.02 $_{av}$	12500.28 $_{av}$		L114 (L111)
	5	**115-321**	23397.64 $_{av}$	23396.86 $_{av}$	23395.16 $_{av}$		L114 (L111)
		1-321	35880.86 $_{av}$	35878.9 $_{av}$	35878.10 $_{av}$	35878.40 $_{av}$	
		1-114	12501.23 $_{av}$	12501.02 $_{av}$	12500.67 $_{av}$	12500.50 $_{av}$	L114 (L111)
	15	**8-114**	11662.74 $_{av}$	11662.28 $_{av}$			

		115-198	9535.62 $_{av}$	9535.21 $_{av}$			
		115-321	23397.64 $_{av}$	23396.86 $_{av}$	23395.43 $_{av}$	23396.90 $_{av}$	L114 (L111)
		1-321	35880.86 $_{av}$	35879.50 $_{av}$	35878.67 $_{av}$	35879.30 $_{av}$	
	30	**1-114**	12501.23 $_{av}$	12500.86 $_{av}$	12500.80 $_{av}$	12501.00 $_{av}$	L114 (L111)
		8-114	11662.74 $_{av}$	11662.11 $_{av}$			
		115-198	9535.62 $_{av}$	9534.35 $_{av}$			
		115-321	23397.64 $_{av}$	23395.91 $_{av}$	23395.60 $_{av}$	23396.73 $_{av}$	L114 (L111)
		1-321	35880.86 $_{av}$	35878.5 $_{av}$	35878.40 $_{av}$	35879.72 $_{av}$	
	60	**1-114**	12501.23 $_{av}$	12500.20 $_{av}$	12500.10 $_{av}$	12500.50 $_{av}$	L114 (L111)
		8-114	11662.74 $_{av}$	11661.99 $_{av}$			
		21-114	10391.8 $_{av}$	10391.27 $_{av}$			
		115-198	9535.62 $_{av}$	9535.12 $_{av}$			
		115-321	23397.64 $_{av}$	23395.8 $_{av}$	23395.80 $_{av}$	23396.80 $_{av}$	L114 (L111)
		1-321	35880.86 $_{av}$	35878.70 $_{av}$	35878.60 $_{av}$	35879.15 $_{av}$	
PET 1:1000	**5**	**1-12**	1297.78 $_{mi}$	1297.76 $_{mi}$			A12 (A9)
		1-14	1467.88 $_{mi}$	1467.85 $_{mi}$			A14 (A11)

		13-321	34600.25 $_{av}$	34597.6 $_{av}$			A12 (A9)
		15-321	34430.43 $_{av}$	34428.2 $_{av}$			A14 (A11)
		1-321	35880.86 $_{av}$	35877.5 $_{av}$	35877.10 $_{av}$	35876.90 $_{av}$	
		1-12	1297.78 $_{mi}$	1297.75 $_{mi}$			A12 (A9)
		1-14	1467.88 $_{mi}$	1467.87 $_{mi}$			A14 (A11)
		1-20	2126.13 $_{mi}$	2126.10 $_{mi}$			L20 (L17)
	15	**13-321**	34600.25 $_{av}$	34598.3 $_{av}$			A12 (A9)
		15-321	34430.43 $_{av}$	34429.0 $_{av}$			A14 (A11)
		21-321	33771.43 $_{av}$	33768.5 $_{av}$			L20 (L17)
		1-321	35880.86 $_{av}$	35878.6 $_{av}$	35878.30 $_{av}$	35879.10 $_{av}$	
		1-12	1297.78 $_{mi}$	1297.77 $_{mi}$			A12 (A9)
		1-14	1467.88 $_{mi}$	1467.86 $_{mi}$			A14 (A11)
		1-20	2126.13 $_{mi}$	2126.11 $_{mi}$	2126.20 $_{mi}$	2126.14 $_{mi}$	L20 (L17)
	30	**13-321**	34600.25 $_{av}$	34596.8 $_{av}$			A12 (A9)
		15-321	34430.43 $_{av}$	34427.4 $_{av}$			A14 (A11)
		21-321	33771.43 $_{av}$	33767.9 $_{av}$	33769.20 $_{av}$	33768.50 $_{av}$	L20 (L17)

		1-321	35880.86 $_{av}$	35876.9 $_{av}$	35878.50 $_{av}$	35877.60 $_{av}$	
		1-12	1297.78 $_{mi}$	1297.80 $_{mi}$			A12 (A9)
		1-14	1467.88 $_{mi}$	1467.87 $_{mi}$			A14 (A11)
		1-20	2126.13 $_{mi}$	2126.12 $_{mi}$	2125.99 $_{mi}$	2126.10 $_{mi}$	L20 (L17)
	60	**13-321**	34600.25 $_{av}$	34599.1 $_{av}$			A12 (A9)
		15-321	34430.43 $_{av}$	34429.5 $_{av}$			A14 (A11)
		21-321	33771.43 $_{av}$	33770 $_{av}$	33768.90 $_{av}$	33770.80 $_{av}$	L20 (L17)
		1-321	35880.86$_{av}$		35877.80 $_{av}$	35880.20 $_{av}$	